BioMACROMOLECULES

Subscriber access provided by University of South Dakota

Article

Use of light-degradable aliphatic polycarbonate nanoparticles as drug carrier for photosensitizer

Jingjiang Sun, Wolfgang Birnbaum, Juliane Anderski, Marie-Theres Picker, Dennis Mulac, Klaus Langer, and Dirk Kuckling

Biomacromolecules, **Just Accepted Manuscript** • DOI: 10.1021/acs.biomac.8b01446 • Publication Date (Web): 15 Nov 2018

Downloaded from http://pubs.acs.org on November 15, 2018

Just Accepted

"Just Accepted" manuscripts have been peer-reviewed and accepted for publication. They are posted online prior to technical editing, formatting for publication and author proofing. The American Chemical Society provides "Just Accepted" as a service to the research community to expedite the dissemination of scientific material as soon as possible after acceptance. "Just Accepted" manuscripts appear in full in PDF format accompanied by an HTML abstract. "Just Accepted" manuscripts have been fully peer reviewed, but should not be considered the official version of record. They are citable by the Digital Object Identifier (DOI®). "Just Accepted" is an optional service offered to authors. Therefore, the "Just Accepted" Web site may not include all articles that will be published in the journal. After a manuscript is technically edited and formatted, it will be removed from the "Just Accepted" Web site and published as an ASAP article. Note that technical editing may introduce minor changes to the manuscript text and/or graphics which could affect content, and all legal disclaimers and ethical guidelines that apply to the journal pertain. ACS cannot be held responsible for errors or consequences arising from the use of information contained in these "Just Accepted" manuscripts.

ACS Publications

is published by the American Chemical Society. 1155 Sixteenth Street N.W., Washington, DC 20036

Published by American Chemical Society. Copyright © American Chemical Society. However, no copyright claim is made to original U.S. Government works, or works produced by employees of any Commonwealth realm Crown government in the course of their duties.

Use of light-degradable aliphatic polycarbonate nanoparticles as drug carrier for photosensitizer

Jingjiang Sun[†,‖], *Wolfgang Birnbaum*[†], *Juliane Anderski*[‡], *Marie-Theres Picker*[†], *Dennis Mulac*[‡], *Klaus Langer*[‡], *Dirk Kuckling*[†]*

[†]Paderborn University, Department of Chemistry, Warburger Str. 100, D-33098 Paderborn, Germany

[‡]University of Münster, Institute of Pharmaceutical Technology and Biopharmacy, Corrensstr. 48, D-48149 Münster, Germany

[‖] Qingdao University of Science and Technology, School of Polymer Science and Engineering, Zhengzhou Rd. 53, CN-266042 Qingdao, China

ABSTRACT:

Aliphatic poly(carbonate)s (APCs) with rapid and controlled degradation upon specific stimulation have great advantages for a variety of biomedical and pharmaceutical applications. In the present work, we reported a new poly(trimethylene carbonate) (PTMC)-based copolymer containing multiple 4,5-dimethoxy-2-nitrobenzyl photo cleavable groups as pendent chains. The six-membered light-responsive cyclic carbonate monomer (**LrM**) was first prepared from 2-(hydroxymethyl)-2-methylpropane-1,3-diol and 4,5-dimethoxy-2-nitrobenzyl alcohol, and then copolymerized with trimethylene carbonate (TMC) by 1,8-diazabicyclo(5.4.0)undec-7-ene (DBU) catalyzed ring-opening polymerization (ROP) to afford the light-responsive polycarbonate

(**LrPC**). The light-triggered decomposition of **LrM** and **LrPC** was studied by NMR, UV/VIS spectroscopy, size exclusion chromatography (SEC), as well as ESI-ToF mass spectrometry (ESI-ToF-MS). Stable monodisperse nanoparticles with hydrodynamic diameter of 100 nm could be formulated from 25% **LrPC** and 75% poly(lactic-*co*-glycolic acid) (PLGA) and applied for the encapsulation of temoporfin. Upon irradiation with UV light these particles displayed a significant decrease of the particle countrate and increased the release rate of temoporfin in comparison to standard PLGA nanoparticles. This work demonstrated that combination of encapsulation of photosensitizer and light degradation using light-responsive polymers is suitable to enhance photodynamic therapy (PDT).

INTRODUCTION

In recent years, aliphatic polycarbonates (APCs) have been intensively studied and used as materials in the biomedical and pharmaceutical fields due to their low toxicity, good biocompatibility and biodegradability.[1-3] In contrast to other approaches to obtain APCs, such as polycondensation of diols with dialkyl carbonates[4-6] and copolymerization of CO_2 and epoxides[7,8], the ring-opening polymerization (ROP) is the most important method to synthesize functionalized APCs with controlled molar masses and polymer structures[9-12]. Although the degradation rates of APCs could be accelerated under acid, basic or enzymatic environment, the controlled degradation of APCs upon internal or external stimuli, such as pH[13-15], temperature[16,17], oxidation[18-20], enzyme[11] and light[21-23], is of great interest for their biomedical applications, such as drug or gene delivery systems. Among various stimuli, the degradation rate of light-responsive polymers can be controlled by adjusting light wavelength, intensity or duration of the irradiation, while other

stimuli (e.g. pH, oxidation) only provide limited control and acceleration of the decomposition process over the time.[24,25]

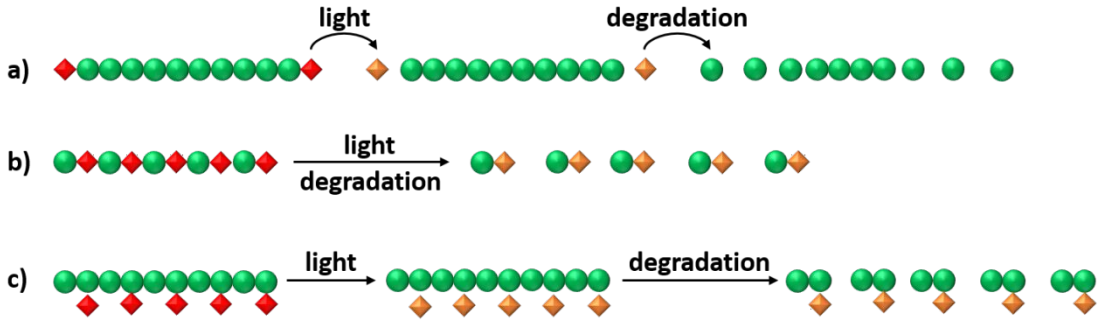

Figure 1. Illustration of different light-responsive degradation systems: a) light-responsive groups end-capped polymers; b) polymers with light-responsive linkers along the polymer backbone; c) polymers with light-responsive pendent groups.

The light-responsive self-immolative polymers can be divided into three classes (**Figure 1**): a) Polymer backbones are end-capped with light-responsive groups, which can lead to a fast degradation via a cascade of self-immolative reactions upon triggering with light.[26-28] b) Photocleavable linkers as monomers are directly incorporated into polymer backbones e.g. by polycondensation. The degradation of polymers is achieved by cleaving self-immolative linkers.[29,30] c) Light-responsive self-immolative groups are constructed as pendent chains along polymer backbones, whose degradation can be accelerated by intramolecular cyclization.[17,31,32] From the view of biomedical applications, most polymers used in these degradation systems are polyesters, polycarbonates and poly(ester-amide)s. Recently, Almutairi et al. reported a series of novel functional poly(ε-caprolactone)[31], poly(lactide-*co*-glycolide) (PLGA)[32] and quinone-methide[26,30] based polyesters and polyurethanes with light-responsive pendent groups or end

groups. Upon irradiation, these polymers degraded into small molecules completely via an intramolecular cyclization or a quinone-methide self-immolative reaction. Li and Du have prepared oxidation-promoted degradable APCs attached with phenylboronic ester pendent chain via a carbamate linker. The H_2O_2-initiated oxidation led to a consecutive degradation process of cleavage of phenylboronic ester, CO_2-release, formation of free amino pendent group and decomposition of the polymer backbone by intramolecular cyclization.[18,19]

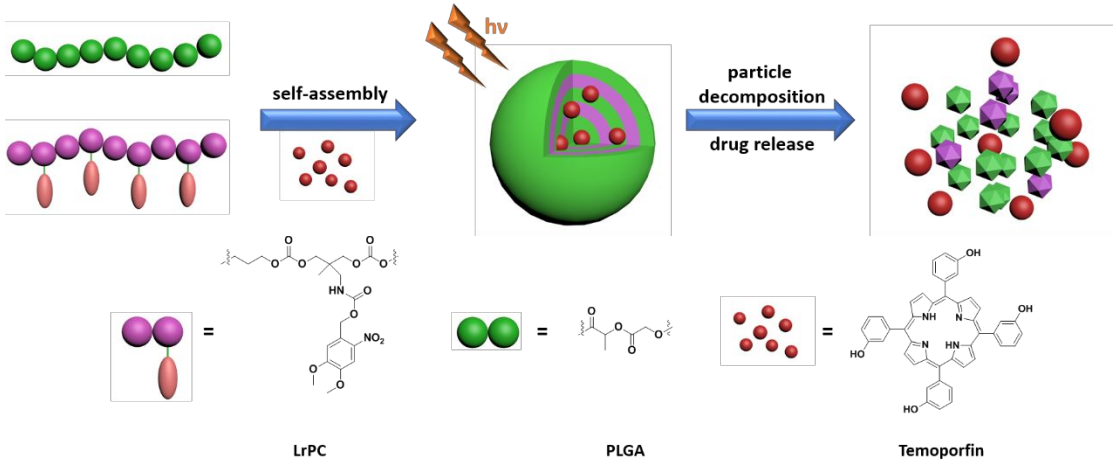

Figure 2. Illustration of the formulation of nanoparticles from **LrPC**, PLGA and temoporfin, and nanoparticle decomposition upon irradiation with UV light.

Photodynamic therapy (PDT) is a novel and efficient option for cancer treatment involving the use of photosensitizers to generate reactive singlet oxygen species upon photoirradiation to destroy tumor cells.[33-35] Efficient anti-tumor photosensitizers are usually highly lipophilic macrocyclic tetrapyrroles, such as porphyrins and chlorins. Due to the high lipophilicity and low water solubility of anti-tumor photosensitizers, there is a need to develop new carriers for efficient load and controlled release of the photosensitizer molecules upon internal or external stimuli.[36-38] To expand the family of light-responsive polymers and their applications, we report a new type of

light-responsive APC which could be used as photosensitizer carrier to combine drug release and PDT together upon irradiation. Toward this aim, a novel six-membered cyclic carbonate monomer (**LrM**) with a light-responsive 4,5-dimethoxy-2-nitrobenzyl pendent group attached via a carbamate linkage was synthesized (**Scheme 1**) and copolymerized with TMC to afford light-responsive copolycarbonate (**LrPC**). By exposure to 300 – 365 nm UV light the photolabile *o*-nitrobenzyl group can be removed according to the redox photoisomerization leading to the release of functional amine group and forming an *o*-nitrosobenzylaldehyde side product.[30] The **LrPC** was stable to air and moisture but decomposed rapidly into small molecules via intramolecular cyclization when the light-responsive pendent groups were cleaved. Furthermore, nanoparticles prepared from 25% of this APC mixed with 75% PLGA are able to significantly increase the release rate of the photosensitizer payload upon irradiation compared to standard PLGA nanoparticles (**Figure 2**).

EXPERIMENTAL SECTION

Materials. Benzyl alcohol (BnOH) (99%, Acros Organics) was distilled over calcium hydride and stored under Ar. Dichloromethane (DCM) (98%, Stockmeier Chemie) was dried over $CaCl_2$ then distilled over calcium hydride. Tetrahydrofuran (THF) (98%, Stockmeier Chemie) was dried over KOH then distilled over calcium hydride. 1,3-dioxan-2-one (TMC) (99%, Shanghai Worldyang Chemical Co.) was purified by column chromatography with ethyl acetate/*n*-hexane (3: 1). The photosensitizer 5,10,15,20-tetrakis(m-hydroxyphenyl) chlorin (*m*THPC, temoprofin) was kindly provided by biolitec research GmbH (Jena, Germany). The polymer poly(DL-lactide-*co*-glycolide) (PLGA), characterized by a copolymer ratio of 50: 50 (Resomer® RG 502H), was purchased from

Evonik Industries (Darmstadt, Germany). Acetone (98%, Stockmeier Chemie), acetonitrile (MeCN) (>99.9%, Carl Roth), ammonium formate (99%, Acros Organics), benzoic acid (>99%, Merck), Celite (Fluka), 1,8-diazabicyclo(5.4.0)undec-7-ene (DBU) (99%, Alfa Aesar), diisopropylethylamine (DIPEA) (99%, Alfa Aesar), dimethylformamide (DMF) (99.9%, Alfa Aesar), 4,5-dimethoxy-2-nitrobenzyl alcohol (DMNA) (98%, Alfa Aesar), 1,4-dioxane (99.8%, Acros Organics), Dulbecco's Modified Eagle Medium (DMEM) (Biochrom AG, Berlin, Germany), ethyl chloroformate (>98%, Fluka), 2-(hydroxymethyl)-2-methylpropane-1,3-diol (97%, Alfa Aesar), fetal bovine serum (FBS) (Biochrom AG, Berlin, Germany), methanol (99.5%, Grüssing), 4-nitrophenyl chloroformate (97%, abcr), Pd/C (10% Pd, Acros Organics), poly(vinyl alcohol) (PVA; average molar mass 30-70 kDa) (Sigma-Aldrich), pyridine (>99%, Alfa Aesar), sodium azide (99%, Acros Organics), *p*-toluenesulfonic acid monohydrate (TsOH) (99%, Merck), 4-toluenesulfonyl chloride (TsCl) (>98%, Merck), triethylamine (TEA) (99%, Acros Organics) were used as received.

Measurements. ^{1}H and ^{13}C nuclear magnetic resonance (NMR) spectra were recorded using Bruker AV 500 spectrometer at 500 MHz and 125 MHz, respectively. Chloroform-*d* ($CDCl_3$-*d*, 99.8 D%) or dimethylsulfoxide-d_6 (DMSO-d_6, 99.8 D%) were used as solvent for NMR measurements. Electrospray ionization time-of-flight (ESI-ToF)-mass spectra were measured on a SYNAPT G2 HDMS ™ from Waters. Data were obtained with Mass Lynx 4.1. Fourier transform infrared (FTIR) spectra were recorded on Vertex 70 spectrometer (Bruker Optik, Ettlingen, Germany) with a RT_DLaTGS Detector. All samples were measured in the wavenumber region of 4,000 cm^{-1} to 400 cm^{-1}. UV/VIS spectra were recorded on Specord 50 PLUS UV/VIS spectrophotometer from Analytik Jena using Aspect UV 1.1 software. The molar masses and dispersities ($Đ_M$) were analyzed employing a size exclusion chromatography (SEC) system

(advanced polymer chromatography from Waters) equipped with two consecutive columns (Acquity APC XT columns filled with polyethoxysilane with a defined porosity of 125 Å and 45 Å, respectively) and an Acquity APC RI-detector. The system was operated at a flow rate of 0.7 mL/min with THF/DMF (v/v = 80/20) as solvents. Poly(methyl methacrylate) (PMMA) standards were used for calibration. Differential scanning calorimetry (DSC) was performed with Netzsch DSC 204 F1 Phönix at a heating rate of 10 K min^{-1} under a nitrogen atmosphere. The glass transition temperature (T_g), melting point (T_m) and decomposition temperature ($T_{dec.}$) were determined with NETZSCH Proteus 6.1.0B. Melting point was measured by employing Büchi Melting Point B-545. Light degradation experiments were performed using an OmniCure S1500 Curing System from Lumen Dynamics with a power of 0.607 W/cm^2 (320 to 480 nm). Nanoparticle sizes and polydispersities (PDI) were measured by photon correlation spectroscopy (PCS) using a Malvern Zetasizer Nano ZS system. Drug load of the nanoparticles as well as drug release were analyzed via high performance liquid chromatography (HPLC-DAD system, Agilent Technologies 1200 series). Freeze-drying was performed in an Epsilon 2-4 single chamber-system (Martin Christ, Osterode am Harz, Germany).

Synthesis of light-responsive cyclic carbonate monomer (LrM) (Scheme 1).

*Synthesis of (2,2,5-trimethyl-1,3-dioxan-5-yl)methanol (**1**)*

1 was synthesized according to the literature.[39] 2-(Hydroxymethyl)-2-methylpropane-1,3-diol (80 g, 0.67 mol), acetone (320 mL), and TsOH (100 mg, 0.53 mmol) were stirred overnight at room temperature. The reaction was quenched by addition of TEA (150 µL, 1.1 mmol). The organic solvent was removed under reduced pressure and the residue was dissolved in DCM

(200 mL). The precipitate was filtered off, the DCM was removed under reduced pressure, and the residue was distilled at 0.2 mbar to achieve 86 g of a slightly viscous liquid (yield = 81%).

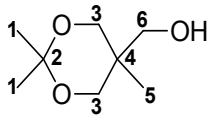

(**Figure S1**)

^{1}H-NMR (500 MHz, $CDCl_3$): δ (ppm) = 0.82 (s, 3 H, $^{5}CH_3$), 1.39 (s, 3 H, $^{1}CH_3$), 1.43 (s, 3 H, $^{1}CH_3$), 1.92 (m, 1 H, OH), 3.60 (m, 2 H, $^{3}CH_2$), 3.67 (m, 2 H, $^{3}CH_2$), 3.68 (s, 2 H, $^{6}CH_2$). ^{13}C-NMR (125 MHz, $CDCl_3$): δ (ppm) = 17.70 (1 C, $^{5}CH_3$), 20.33 (1 C, $^{1}CH_3$), 27.33 (1 C, $^{1}CH_3$), 34.87 (1 C, $^{4}C_q$), 66.01 (1 C, $^{6}CH_2$), 66.46 (2 C, $^{3}CH_2$), 98.10 (1 C, $^{2}C_q$).

*Synthesis of (2,2,5-trimethyl-1,3-dioxan-5-yl)methyl 4-methylbenzenesulfonate (**2**)*

2 was synthesized according to the literature.[40] A solution of TsCl (108 g, 0.57 mol) in pyridine (140 mL) was dropped over 30 min to a solution of **1** (86 g, 0.54 mol) in pyridine (270 mL). The resulting solution was stirred for 40 min at 100 °C, cooled and poured in an excess of ice water. The precipitate was collected, washed with water and dried *in vacuo* to yield 140 g of an off-white solid (yield = 83%). The crude product was used without further purification in the next step.

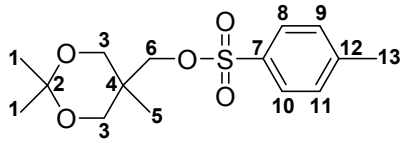

(**Figure S2**)

^{1}H-NMR (500 MHz, $CDCl_3$): δ (ppm) = 0.81 (s, 3 H, $^{5}CH_3$), 1.22 (s, 3 H, $^{1}CH_3$), 1.36 (s, 3 H, $^{1}CH_3$), 2.43 (s, 3 H, $^{13}CH_3$), 3.54 (s, 4 H, $^{3}CH_2$), 4.07 (s, 2 H, $^{6}CH_2$), 7.34 (d, $^{3}J_{HH}$ = 8.3 Hz, 2 H, ^{9,11}CH), 7.79 (d, $^{3}J_{HH}$ = 8.3 Hz, 2 H, ^{8,10}CH). ^{13}C-NMR (125 MHz, $CDCl_3$): δ (ppm) = 17.34 (1 C, $^{5}CH_3$), 19.50 (1 C, $^{1}CH_3$), 21.72 (1 C, $^{13}CH_3$), 27.71 (1 C, $^{1}CH_3$), 34.06 (1 C, $^{4}C_q$), 65.65 (2 C,

$^{3}CH_2$), 72.61 (1 C, $^{6}CH_2$), 98.18 (1 C, $^{2}C_q$), 128.18 (2 C, $^{8,10}CH$), 129.94 (2 C, $^{9,11}CH$), 132.85(1 C, $^{7}C_q$), 144.87 (1 C, $^{12}C_q$).

*Synthesis of 5-(azidomethyl)-2,2,5-trimethyl-1,3-dioxane (**3**)*

3 was synthesized according to the literature.[41] **2** (37.72 g, 120 mmol), NaN_3 (23.41 g, 360 mmol), water (20 mL) and DMF (200 mL) were stirred at 100 °C for 68 h. The mixture was poured in water and extracted four times with Et_2O (130 mL). The organic phase was dried over anhydrous $MgSO_4$ and the solvent was removed under reduced pressure. The residue was purified by column chromatography with silica gel (100 g) and ethyl acetate/*n*-hexane (1/4) to give 20.9 g of a colorless liquid (yield = 94%).

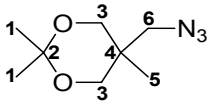

(**Figure S3**)

^{1}H-NMR (500 MHz, $CDCl_3$): δ (ppm) = 0.81 (s, 3 H, $^{5}CH_3$), 1.38 (s, 3 H, $^{1}CH_3$), 1.41 (s, 3 H, $^{1}CH_3$), 3.50 (s, 2 H, $^{6}CH_2$), 3.57 (m, 4 H, $^{3}CH_2$). ^{13}C-NMR (125 MHz, $CDCl_3$): δ (ppm) = 18.13 (1 C, $^{5}CH_3$), 19.81 (1 C, $^{1}CH_3$), 27.73 (1 C, $^{1}CH_3$), 34.55 (1 C, $^{4}C_q$), 56.14 (1 C, $^{6}CH_2$), 66.78 (2 C, $^{3}CH_2$), 98.22 (1 C, $^{2}C_q$).

*Synthesis of (2,2,5-trimethyl-1,3-dioxan-5-yl)methanamine (**4**)*

4 was synthesized similar to the literature.[42] **3** (9.26 g, 50 mmol) and ammonium formate (12.6 g, 200 mmol) were dissolved in dry MeOH (130 mL). The solution was purged with argon for 20 min. The freshly degassed mixture was held under Ar atmosphere while Pd/C (10%) (0.9 g) was added. The reaction mixture was stirred at room temperature in the opened reaction vessel. After a few min the solution became slightly warm and a large gas formation was noticed. From now the reaction mixture was stirred at room temperature for further 4.5 h. Pd/C was removed by

filtration through a pad of Celite and the solvent was removed under reduced pressure. The residue was dissolved in water (25 mL) and the resulting solution was extracted three times with Et_2O (3 x 50 mL). The aqueous phase was basified with KOH (25 g) and extracted five times with MeCN (5 x 25 mL). The organic phase was dried over anhydrous $MgSO_4$ and the solvent was removed under reduced pressure to yield 5.91 g of a colorless liquid (yield = 74%). The crude product was used without further purification in the next step.

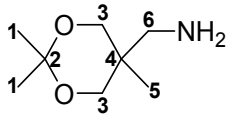

(**Figure S4**)

^{1}H-NMR (500 MHz, $CDCl_3$): δ (ppm) = 0.78 (s, 3 H, $^5CH_3$), 1.21 (b, 2 H, NH_2), 1.36 (s, 3 H, $^1CH_3$), 1.40 (s, 3 H, $^1CH_3$), 2.76 (s, 2 H, $^6CH_2$), 3.58 (m, 4 H, $^3CH_2$). ^{13}C-NMR (125 MHz, $CDCl_3$): δ (ppm) = 17.80 (1 C, $^5CH_3$), 20.97 (1 C, $^1CH_3$), 26.31 (1 C, $^1CH_3$), 34.10 (1 C, ^4C_q), 46.15 (1 C, $^6CH_2$), 67.06 (2 C, $^3CH_2$), 97.64 (1 C, ^2C_q).

*Synthesis of 4,5-dimethoxy-2-nitrobenzyl ((2,2,5-trimethyl-1,3-dioxan-5-yl)methyl)carbamate (**5**)*

A mixture of **4** (2.954 g, 18.55 mmol), **7** (5.965 g, 15.77 mmol), TEA (4.9 mL, 35.16 mmol), and dry MeCN (120 mL) was stirred at room temperature overnight. After adding DCM (100 mL) the organic phase was washed twice with 0.1 M Na_2CO_3 solution (2 x 100 mL) and twice with 0.3 M NaCl solution (2 x 100 mL). The organic phase was dried over anhydrous $MgSO_4$ and the solvent was removed under reduced pressure to yield 7.68 g of a viscous yellow liquid (yield = 84%). The crude product was used without further purification in the next step.

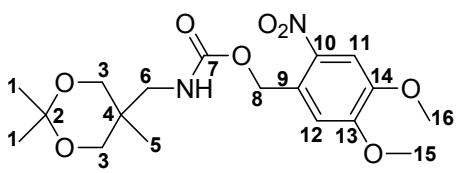

(**Figure S5**)

^{1}H-NMR (500 MHz, $CDCl_3$): δ (ppm) = 0.81 (s, 3 H, $^{5}CH_3$), 1.40 (s, 3 H, $^{1}CH_3$), 1.43 (s, 3 H, $^{1}CH_3$), 3.40 (d, $^{3}J_{HH}$ = 6.1 Hz, 2 H, $^{6}CH_2$), 3.60 (m, 4 H, $^{3}CH_2$), 3.95 (s, 3 H, $O^{15}CH_3$), 3.97 (s, 3 H, $O^{16}CH_3$), 5.22 (b, 1 H, NH), 5.52 (s, 2 H, $^{8}CH_2$), 7.01 (s, 1 H, ^{12}CH), 7.71 (s, 1 H, ^{11}CH).

*Synthesis of 4,5-dimethoxy-2-nitrobenzyl (3-hydroxy-2-(hydroxymethyl)-2-methylpropyl)carbamate (**6**)*

1 N HCl (25 mL) was added to a mixture of **5** (5.465 g, 13.70 mmol) and THF (25 mL). The suspension was stirred at room temperature overnight. After addition of DCM (100 mL) the mixture was washed three times with 0.1 M Na_2CO_3 solution (3 x 100 mL) and twice with 0.3 M NaCl solution (2 x 100 mL). The organic phase was dried over anhydrous $MgSO_4$ and the solvent was evaporated under reduced pressure.

Purification method 1: Et_2O was added to the crude product and stirred/ triturated until a fine precipitate appears. A large excess of Et_2O was reduced before the precipitate was collected by filtration and dried under reduced pressure to achieve 4.326 g of a yellow solid (yield = 88%).

Purification method 2: The crude product was purified by column chromatography with silica gel and ethyl acetate to give 4.410 g of a yellow solid (yield = 90%).

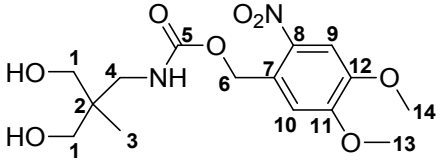

(**Figure S6**)

^{1}H-NMR (500 MHz, DMSO-d_6): δ (ppm) = 0.73 (s, 3 H, $^{3}CH_3$), 2.98 (d, $^{3}J_{HH}$ = 6.3 Hz, 2 H, $^{4}CH_2$), 3.21 (d, $^{3}J_{HH}$ = 5.5 Hz, 4 H, $^{1}CH_2$), 3.87 (s, 3 H, $O^{13}CH_3$), 3.91 (s, 3 H, $O^{14}CH_3$), 4.32 (t, $^{3}J_{HH}$ = 5.5 Hz, 2 H, OH), 5.34 (s, 2 H, $^{6}CH_2$), 7.19 (s, 1 H, ^{10}CH), 7.22 (t, $^{3}J_{HH}$ = 6.2 Hz, 1 H, NH), 7.70 (s, 1 H, ^{9}CH). ^{13}C-NMR (125 MHz, DMSO-d_6): δ (ppm) = 17.08 (1 C, $^{3}CH_3$), 41.36 (1 C, $^{2}C_q$),

44.29 (1 C, $^{4}CH_2$), 56.22 (1 C, $O^{13}CH_3$), 56.32 (1 C, $O^{14}CH_3$), 62.44 (1 C, $^{6}CH_2$), 64.55 (2 C, $^{1}CH_2$), 108.32 (1 C, ^{9}CH), 110.64 (1 C, ^{10}CH), 128.11 (1 C, $^{7}C_q$), 139.43 (1 C, $^{8}C_q$), 147.85 (1 C, $^{11}C_q$), 153.48 (1 C, $^{12}C_q$), 156.55 (1 C, $^{5}C_q$). FTIR (cm^{-1}): 3291 (*v*-O-H), 1690 (*v*-C=O, carbamate), 1581 (*v*-C=C, aromatic), 1519 (v_{as}-NO_2), 1319 (v_s-NO_2), 1270 (*v*-C-O, carbamate) and 1223 (*v*-C-O, ether). ESI-ToF-MS (m/z): $[M + Na]^+$ calculated for $C_{15}H_{22}N_2O_8Na^+$, 381.1274; found, 381.1271. Melting point (T_m) = 99.4 °C.

Synthesis of 4,5-dimethoxy-2-nitrobenzyl ((5-methyl-2-oxo-1,3-dioxan-5-yl)methyl)carbamate ***(LrM)***

6 (4.132 g, 11.53 mmol) was suspended in anhydrous THF (30 mL) under Ar atmosphere and cooled to 0 °C. Subsequently, TEA (4.22 mL, 30.45 mmol) and ethyl chloroformate (2.55 mL, 26.65 mmol) were added and the suspension was stirred at room temperature for 24 h. The precipitate was collected, washed with THF (100 mL), stirred in water (100 mL) for 30 min, filtered off, washed twice with water (2 x 100 mL) and three times with Et_2O (3 x 100 mL), and was dried *in vacuo* to afford 4.011 g of an off-white solid (yield = 73%).

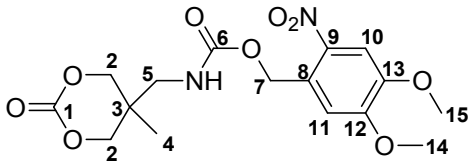

(**Figure S7**)

^{1}H-NMR (500 MHz, DMSO-d_6): δ (ppm) = 0.93 (s, 3 H, $^{4}CH_3$), 3.13 (d, $^{3}J_{HH}$ = 6.4 Hz, 2 H, $^{5}CH_2$), 3.87 (s, 3 H, $O^{14}CH_3$), 3.91 (s, 3 H, $O^{15}CH_3$), 4.12 (d, $^{2}J_{HH}$ = 10.6 Hz, 2 H, $^{2}CH_2$), 4.22 (d, $^{2}J_{HH}$ = 10.6 Hz, 2 H, $^{2}CH_2$), 5.35 (s, 2 H, $^{7}CH_2$), 7.20 (s, 1 H, ^{11}CH), 7.67 (t, $^{3}J_{HH}$ = 6.3 Hz, 1 H, NH), 7.70 (s, 1 H, ^{10}CH). ^{13}C-NMR (125 MHz, DMSO-d_6): δ (ppm) = 16.70 (1 C, $^{4}CH_3$), 32.70 (1 C, $^{3}C_q$), 43.11 (1 C, $^{5}CH_2$), 56.23 (1 C, $O^{14}CH_3$), 56.35 (1 C, $O^{15}CH_3$), 62.74 (1 C, $^{7}CH_2$), 73.90 (2 C,

$^{2}CH_2$), 108.35 (1 C, ^{10}CH), 111.01 (1 C, ^{11}CH), 127.60 (1 C, $^{8}C_q$), 139.60 (1 C, $^{9}C_q$), 147.65 (1 C, $^{1}C_q$), 147.95 (1 C, $^{12}C_q$), 153.39 (1 C, $^{13}C_q$), 156.53 (1 C, $^{6}C_q$). ESI-ToF-MS (m/z) (**Figure S8**): $[M + Na]^+$ calculated for $C_{16}H_{20}N_2O_9Na^+$, 407.1066; found, 407.1066. FTIR (cm^{-1}): 3083 (*v*-C-H, aromatic), 1738 (*v*-C=O, carbonate), 1714 (*v*-C=O, carbamate), 1584 (*v*-C=C, aromatic), 1523 (v_{as}-NO_2), 1322 (v_s-NO_2), 1274 (*v*-C-O, carbamate), 1245 (*v*-C-O, carbonate), 1221 (*v*-C-O, ether). Melting point (T_m) = 192.5 °C.

Synthesis of 4,5-dimethoxy-2-nitrobenzyl(4-nitrophenyl)carbonate (7)

7 was synthesized according to the literature.[30] DIPEA (15 mL, 86.11 mmol) was added dropwise to a mixture of DMNA (8.80 g, 41.28 mmol), 4-nitrophenyl chloroformate (15.55 g, 77.15 mmol) and DCM (90 mL) under Ar atmosphere. The solution was stirred at room temperature for 1.5 h and was then diluted with DCM (90 mL). After stirring at room temperature overnight the solvent was removed under reduced pressure. The resulting product was suspended in ethanol (290 mL) and heated to 85 °C for 45 min until a fine precipitate was formed. The precipitate was collected and dried *in vacuo* to afford 14.16 g of a yellowish solid (yield = 91%).

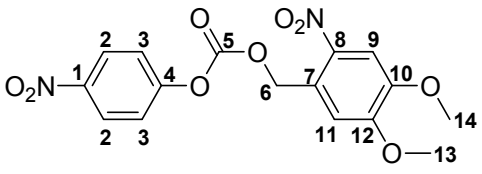

(**Figure S9**)

^{1}H-NMR (500 MHz, DMSO-d_6): δ (ppm) = 3.89 (s, 3 H, $O^{13}CH_3$), 3.92 (s, 3 H, $O^{14}CH_3$), 5.61 (s, 2 H, $^{6}CH_2$), 7.26 (s, 1 H, ^{11}CH), 7.59 (d, $^{3}J_{HH}$ = 9.1 Hz, 2 H, ^{3}CH), 7.73 (s, 1 H, ^{9}CH), 8.33 (d, $^{3}J_{HH}$ = 9.1 Hz, 2 H, ^{2}CH). ^{13}C-NMR (125 MHz, DMSO-d_6): δ (ppm) = 56.14 (1 C, $O^{13}CH_3$), 56.32 (1 C, $O^{14}CH_3$), 67.22 (1 C, $^{6}CH_2$), 108.30 (1 C, ^{9}CH), 112.00 (1 C, ^{11}CH), 122.57 (2 C, ^{3}CH), 124.37

(1 C, $^{7}C_q$), 125.45 (2 C, ^{2}CH), 139.04 (1 C, $^{8}C_q$), 145.25 (1 C, $^{1}C_q$), 148.40 (1 C, $^{12}C_q$), 151.62 (1 C, $^{5}C_q$), 153.17 (1 C, $^{10}C_q$), 155.17 (1 C, $^{4}C_q$).

General procedure for the synthesis of light-responsive (co)polycarbonate (LrPC) by ROP. Take the preparation of **LrPC-2** (**Table 1**) as an example. In a Schlenk tube, **LrM** (0.461 g, 1.20 mmol), TMC (0.123 g, 1.20 mmol) and BnOH (4,16 μL, 0.04 mmol) were suspended in dry 1,4-dioxane (2 mL) under Ar atmosphere. After adding DBU (9.06 μL, 0.06 mmol) the reaction mixture was stirred at 80 °C for 22 h and was then quenched by adding benzoic acid (10 mg, 0.07 mmol). The polymer was purified by precipitation into Et_2O and dried *in vacuo* to give a yellow solid (yield = 73%).

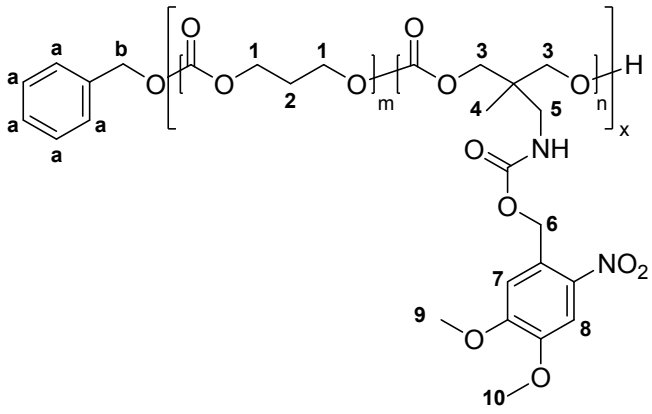

(**Figure S10**)

^{1}H-NMR (500 MHz, DMSO-d_6): δ (ppm) = 0.70 – 1.00 (m, 3 H, $^{4}CH_3$), 1.80 – 2.00 (m, 2 H, $^{2}CH_2$), 2.90 – 3.10 (m, 2 H, $^{5}CH_2$), 3.75 – 4.00 (m, 3 H, $O^{9}CH_3$; 3 H, $O^{10}CH_3$; 4 H, $^{3}CH_2$), 4.00 – 4.25 (m, 4 H, $^{1}CH_2$), 5.11 (s, 2 H, $^{b}CH_2$), 5.25 – 5.40 (m, 2 H, $^{6}CH_2$), 7.00 – 7.85 (m, 1 H, NH; 2 H, $^{7,8}CH$; 5 H, ^{a}CH). FTIR (cm^{-1}): 1749 (ν-C=O, carbonate and carbamate), 1584 (*ν*-C=C, aromatic), 1525 (ν_{as}-NO_2), 1330 (ν_{s}-NO_2), 1281 (*ν*-C-O, carbamate), 1241 (*ν*-C-O, carbonate), 1221 (*ν*-C-O, ether).

Kinetic of ring-opening (co)polymerization. For kinetic investigation, the (co)polymerization was conducted by the same procedure aforementioned. At specific times, 0.1 mL of the reaction

mixture was taken out, quenched by adding benzoic acid and studied by ^{1}H NMR spectroscopy. Conversions of **LrM** and TMC were calculated from the relative integrals of the monomer (2.05 ppm for TMC and 3.25 ppm for **LrM**) and copolymer (1.95 ppm for PTMC and 3.11 ppm for **LrPC**) peaks in ^{1}H NMR spectra (**Figure S11**).

Light decomposition of LrM followed by ESI-ToF-MS. DCM (3 mL) containing **LrM** (5 mg) (1.67 mg/mL) was charged into a vial, and then irradiated with UV light (0.607 W/cm^2, 320 – 480 nm) for 15 min. After removing the DCM under reduced pressure, the degradation products were studied by ESI-ToF-MS.

Light responsiveness of LrPC-2 monitored by UV/VIS spectrophotometer. A polymer solution of **LrPC-2** was prepared in DCM (0.075 mg/mL). The **LrPC-2** solution was irradiated in a quartz cuvette with UV light (0.607 W/cm^2, 320 – 480 nm) for the specified periods of time (up to 180 s). UV/VIS absorbance spectra were recorded after each irradiation.

Light degradation of LrPC-2 followed by SEC. Five polymer solutions of **LrPC-2** were prepared in SEC vials in THF (2 mg/mL). These samples were irradiated with UV light (0.607 W/cm^2, 320 – 480 nm) for the specified times of 0, 1, 5, 15, and 30 min, and then analyzed by SEC.

Light degradation of LrPC-2 followed by ^{1}H NMR spectroscopy. LrPC-2 (7.5 mg) was dissolved in DMSO-d_6 (0.5 mL) (15 mg/mL). The **LrPC** solution was irradiated directly in vial with UV light (0.607 W/cm^2, 320 – 480 nm) for 15 min and ^{1}H NMR spectra before and after irradiation were taken.

Nanoparticle preparation, lyophilization, and characterization. Nanoparticles (NP) with a hydrodynamic diameter of about 100 nm were prepared using a solvent displacement preparation

technique. In brief, **LrPC-2** (7.5 mg) and PLGA (22.5 mg) were dissolved in acetone (1 mL), respectively. After combining both organic solutions, the photosensitizer temoporfin (*m*THPC) (3 mg) was added and dissolved. The organic solution was injected into an aqueous PVA solution (2% (w/v)) (4 mL). The nanoparticle suspension was stirred overnight, whereby evaporation of the organic solvent led to the final particle formation. Afterwards, purification of the nanoparticle suspension was conducted three times via centrifugation (30,000 g, 1.5 h) and redispersion in water. The NP were referred to as *m*THPC-LrPC-PLGA-NP. To obtain unloaded NP (LrPC-PLGA-NP) the preparation process was performed in the absence of the photosensitizer.

Temoporfin loaded nanoparticle suspensions were freeze-dried in the presence of 3% trehalose using the following parameters: Freezing at -40 °C for 7 h, a primary drying step at -34 °C and a vacuum of 0.05 mbar for 40 h, followed by a secondary drying phase at 20 °C and 0.025 mbar for 11 h.

The amount of the particle incorporated *m*THPC was determined by dissolving nanoparticles (1 mg) in acetone (1 mL). The released photosensitizer was quantified via HPLC with the aid of a calibration curve of pure *m*THPC (concentration range from 10 to 100 µg/mL). A reversed phase column (Gemini RP 18, 250 x 4.6 mm, particle diameter 5 µm, Phenomenex Inc., Aschaffenburg, Germany) was used. An isocratic elution was performed at a flow rate of 1.0 mL/min. The mobile phase consisted of 42.5% water with 0.1% (w/v) trifluoroacetic acid and 57.5% acetonitrile. The photosensitizer was detected at a wavelength of 415 nm.

Light-induced nanoparticle decomposition. Light-depending particle degradation was investigated after illumination of a diluted nanoparticle suspension (0.1 mg NP/mL suspension) with light of a wavelength of 365 nm (Thorlabs´ Mounted LED M365LP1, 1,150 mW, Ø57.0 mm,

1.76 mW/cm^2) for 5 min. Variations in the count rate of the nanoparticle suspensions were observed over 24 h via PCS measurements at a temperature of 22 °C and a backscatter angle of 173°. In between the measurements, samples were stored in the dark at room temperature. All measurements were performed with unloaded nanoparticles.

Photosensitizer temoporfin release. The temoporfin release kinetics were determined by first dispersing lyophilized nanoparticles in Dulbecco's Modified Eagle Medium (DMEM) containing 10% (v/v) fetal bovine serum (FBS) at a concentration of 0.4 mg NP/mL. Afterwards, aliquots of 1 mL were irradiated for 5 min with light of a wavelength of 365 nm and afterwards incubated at 37 °C for defined times (15 min, 30 min, 60 min, 2 h, 4 h, 6 h, 24 h). The collected samples were centrifuged (30,000 g, 15 min) and the supernatants were collected. 150 µL of each supernatant was mixed with acetone (450 µL) to precipitate remaining serum protein and to dissolve the drug. In a further centrifugation step (20,000 g, 10 min), the precipitated proteins were separated and the photosensitizer content of the supernatants was determined via HPLC-FLD analysis. The HPLC-parameters were the same as described above, except that released *m*THPC was detected with a fluorescence detector at 421 nm excitation and 653 nm emission wavelength.

Atomic force microscopy (AFM) measurements. The visualization of the NP was performed by AFM employing a Bruker Dimension 3100 atomic force microscope, equipped with a Nanoscope IIIa controller (Bruker, Karlsruhe, Germany) before and after illumination of the NP suspensions. Samples were prepared as follows: NP suspensions were diluted to a concentration of 0.16 mg NP/mL. An aliquot (3 µL) of the NP suspension was pipetted on a specimen slide and dried under a darkened fume cupboard. The remaining NP suspension was illuminated for 5 min with light of a wavelength of 365 nm and stored for 24 h in the dark at room temperature. Afterwards, 3 µL of

the treated NP suspension was pipetted on a second specimen slide and also dried under a darkened fume cupboard until AFM measurements were conducted.

AFM measurements were performed in intermittent contact mode (Tapping Mode®) with n-type silicon cantilevers (HQ:NSC14/Al BS, nominal tip radius < 10 nm, typical resonant frequency of about 160 kHz and a nominal spring constant of 5 N/m; manufactured by µmash, Sofia, Bulgaria), 2% below resonance frequency at a RMS amplitude of around 2. Further data analysis was carried out using Nanoscope analysis software version 1.5.

RESULTS AND DISCUSSION

Synthesis and characterization of LrM. The six-membered cyclic carbonate monomer **LrM** was prepared from 2-(hydroxymethyl)-2-methylpropane-1,3-diol following the synthetic route as shown in **Scheme 1**. In a four-step reaction one hydroxy group (**1**) was converted into an amino group (**4**).[39-42] Amine **4** was then protected with the light-cleavable 4,5-dimethoxy-2-nitrobenzyl group via a carbamate linkage to give compound **5**. The acetal **5** was hydrolyzed with HCl to reveal the diol **6**, which was cyclized with ethyl chloroformate to form the cyclic **LrM**. The overall yield for **LrM** was 29% over seven steps. The structure of **LrM** was confirmed by NMR spectroscopy (**Figure S7**) and ESI-ToF-MS (**Figure S8**). The **LrM** possess poor solubility (only soluble in DMSO and DMF at room temperature) and very high melting point, which were probably caused by strong intermolecular hydrogen bonding (**Figure S12**) between carbamate and carbonate groups due to the presence of the electron withdrawing *o*-nitrobenzyl group. In addition, based on the

DSC measurement (**Figure S13**) the melting point (T_m) and decomposition temperature ($T_{dec.}$) of **LrM** were found to be 193 °C and 202 °C, respectively.

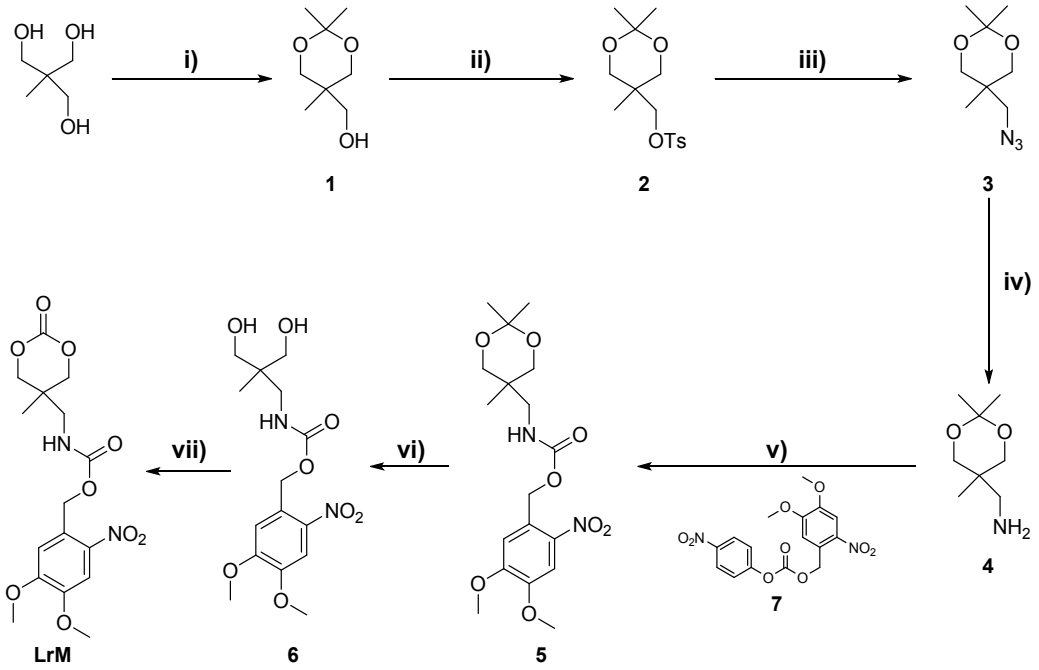

Scheme 1. Synthetic route for **LrM**. Reagents and conditions: i) acetone, TsOH, rt, 20 h; ii) TsCl, pyridine, rt, 30 min → 100 °C, 40 min; iii) NaN_3, DMF/H_2O (10/1), 68 h, 100 °C; iv) ammonium formate, Pd/C, MeOH, rt, 4 h; v) **7**, TEA, MeCN, rt, overnight; vi) THF/1 N HCl (1/1), rt, overnight; vii) ethyl chloroformate, TEA, THF, 0 °C → rt, overnight.

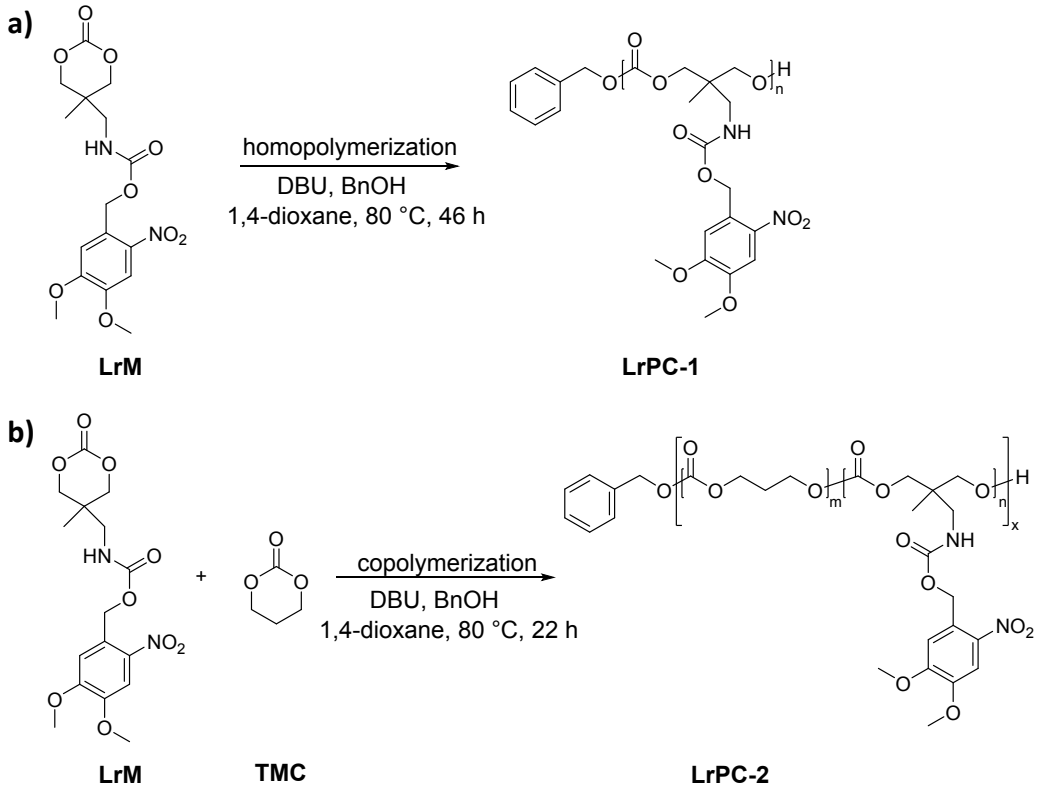

Scheme 2. Preparation of the light-responsive homopolymer (a) and copolymer (b) by ROP in 1,4-dioxane using DBU as catalyst and BnOH as initiator.

Synthesis of light-responsive (co)polycarbonate by ROP. ROP of cyclic carbonate monomers catalyzed by organo-catalysts, such as DBU, 1,5,7-triazabicyclo[4.4.0]dec-5-ene (TBD) and (-)-sparteine, have been intensively investigated and proved to be efficient method for the APC preparation.[43-45] We attempted to synthesize light-responsive homo- and copolycarbonates by employing DBU as organo-catalyst and BnOH as initiator for the ROP of **LrM** (**Scheme 2**). Attempts of ROP at room temperature in various aprotic organic solvents were unsuccessful due to the poor solubility of **LrM**. Through optimizing the polymerization conditions, we found that **LrM** could be polymerized in 1,4-dioxane at 80 °C. First, the kinetic of homopolymerization of

LrM was investigated and followed by proton NMR spectroscopy. As shown in **Figure 3a** and **b**, **LrM** was polymerized very slowly with polymerization rate constants of 0.0138 h^{-1} (0 – 22 h) and 0.0256 h^{-1} (22 – 46 h), respectively (**Figure S14 a** and **b**). The monomer conversion reached only 64% after 46 h. During the polymerization, the mixture remained in the suspension state, strongly limiting the polymerization rate and conversion. The final number averaged molar mass (M_n) of the obtained homopolycarbonate (**LrPC-1**) was 2,200 g/mol with dispersity ($Đ_M$) of 1.23 (**Table 1**).

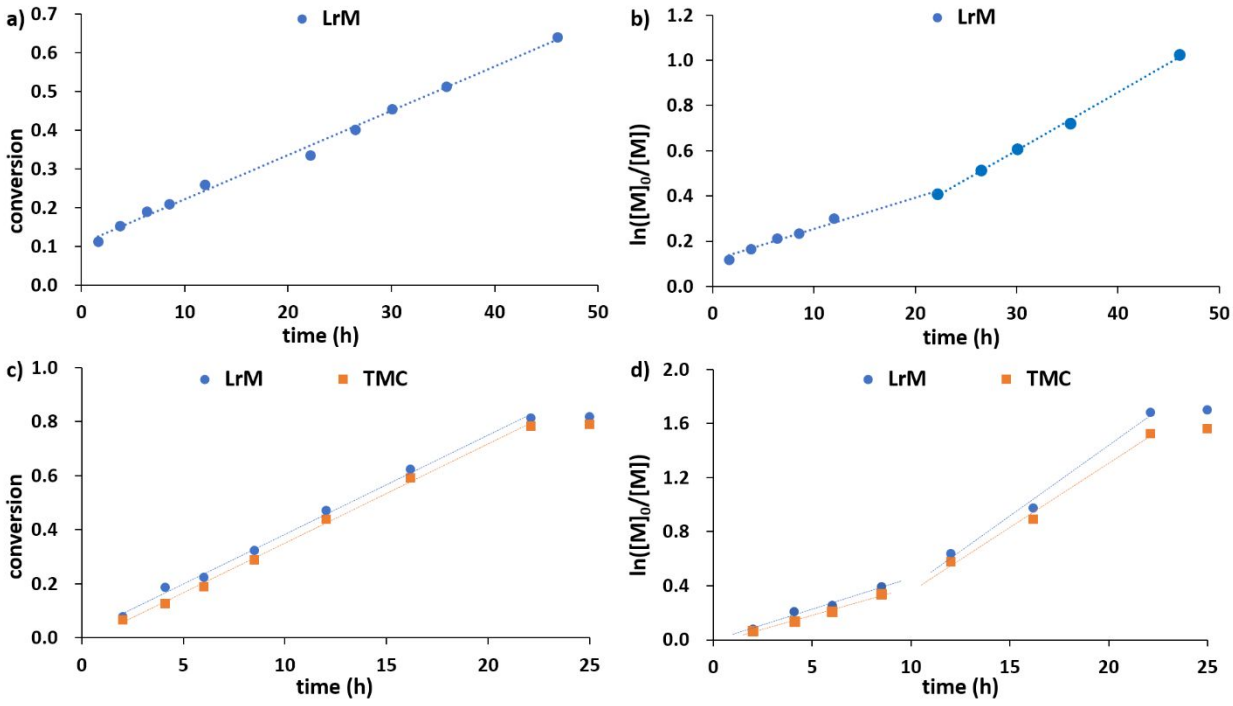

Figure 3. Kinetics of homopolymerization of **LrM** (a and b) and copolymerization of **LrM** with TMC (c and d) catalyzed by DBU and initiated by BnOH at 80 °C.

Copolymerization is a facile method to provide the opportunity to modify polymer properties. To increase the molar masses of obtained polymers, we further attempted the copolymerization of

LrM and commercially available TMC with a molar feed ratio of 1: 1 (**Scheme 2b**). Fortunately, the solubility of the monomer mixture containing 50% TMC was significantly enhanced, because TMC could form new single hydrogen bonding with the carbamate group instead of double hydrogen bonding between **LrMs**, thereby changing the hydrogen bonding system and leading to a faster polymerization rate. Initially, we thought that for the copolymerization of **LrM** and TMC a pseudo-block copolymer, PTMC-*b*-LrPC, could be obtained, since TMC has a very high ROP rate catalyzed by DBU, as previously reported[46]. However, the kinetic analysis (**Figure 3c** and **d**) suggested that TMC and **LrM** were polymerized at similar rates leading to a statistic copolymer. In the first 8.5 h, due to the poor monomer solubility the ROP of both **LrM** and TMC showed slower rate constants of 0.0460 h^{-1} and 0.0417 h^{-1} for **LrM** and TMC, respectively. As the polymerization proceeded, the polymerization rate increased to 0.1045 h^{-1} and 0.0949 h^{-1} for **LrM** and TMC (**Figure S14c** and **d**), respectively, with the increase of the monomer solubility in polycarbonate solution. The suspension cleared after 20 h, and maximal conversion of 80% for both monomers was reached after 22 h, thereafter, their conversions remained unchanged. According to the previous reports by Endo et al.[47,48] the ROP equilibrium of some 5,5-disubstituted TMC could be strongly affected by polymerization temperature. The higher the polymerization temperature, the lower the maximal monomer conversion that could be reached. The final copolycarbonate had M_n of 4,400 g/mol and $Đ_M$ of 1.47. The thermal properties of **LrPC-2** were investigated by DSC (**Figure S13**). The glass transition temperature (T_g), T_m and $T_{dec.}$ were detected at 41 °C, 64 °C and 166 °C, respectively. Moreover, the thermal and hydrolytic stability of **LrPC-2** was studied in DMSO-d_6/D_2O (v/v = 5/1, 16.7 mg/mL) solution at 37 °C by ^{1}H NMR spectroscopy. As shown in **Figure S15**, both chemical shifts and relative intensities of polymer

signals in ^{1}H NMR spectra remained unchanged up to 21 days incubation at 37 °C pointing out the excellent stability of **LrPC-2**.

Table 1. Results of the synthesis of homo- and copolycarbonates by ROP of **LrM**.

	[LrM]:[TMC]:[I][a]	$M_{n,th}$[b] (g/mol)	t (h)	conv.[c] (%) LrM	conv.[c] (%) TMC	DP[d] (LrM + TMC)	$M_{n,SEC}$[e] (g/mol)	$Đ_M$[e]
LrPC-1	30: 0: 1	7,400	46	64	-	5 + 0	2,200	1.23
LrPC-2	30: 30: 1	11,500	22	81	79	10 + 10	4,400	1.47

[a]Both polymerizations were conducted in 1,4-dioxane at 80 °C using DBU as the organo-catalyst and BnOH as the initiator. [b]$M_{n,th}$ = ([LrM]/[I]) x M(LrM) x conv.(LrM) + ([TMC]/[I]) x M(TMC) x conv.(TMC) + M(BnOH). [c]Determined by ^{1}H NMR spectra of polymer solution (**Figure S11**). [d]Determined by ^{1}H NMR spectra of purified polymers; DP = degree of polymerization. [e]Determined by SEC in THF/DMF (8/2) with PMMA standards.

The copolymerization of **LrM** and TMC appeared to suffer from side reactions, such as transcarbamation, leading to lower M_n than that ($M_{n,th}$) predicted from the molar feed ratio [**LrM**]: [TMC]: [I] and conversion as well as higher $Đ_M$. The possible mechanism of the transcarbamation is shown in **Figure 4a**. Since 4,5-dimethoxy-2-nitrobenzyl group is a strong electron withdrawing group, the carbamate group could be deprotonated by DBU and attacked the carbonate group in polymer backbone via intramolecular cyclization at evaluated temperature leading to polymer fragmentation and loss of expected benzyl alcohol end groups. As a result of the transcarbamation a small signal at 5.42 ppm corresponding to the carbamate end group (**e'**) could be observed after the ROP, while the CH_2 (**l**) for the benzyl alcohol end group at 5.12 ppm almost disappeared

(**Figure 4b**). Moreover, the ratio of the relative intensities for the NH (**d**, 7.54 ppm) and CH_2 (**e** + **e'**, 5.33 ppm and 5.42 ppm, respectively) groups was found to be 1: 3.02 (**Figure S10**), which was smaller than the ratio in the **LrM** spectrum of 1: 2.27 (**Figure S7**), providing circumstantial evidence for this mechanism. The structure of **LrPC-2** was confirmed by ^{1}H NMR spectroscopy (**Figure 4b**). Comparing the relative intensity at 1.93 ppm for PTMC and 3.07 ppm for **LrPC**, we determined that the final copolycarbonate contained 52% light-responsive part, which was in agreement with the kinetic results. DPs were calculated from the relative integrals of the polymer (1.93 ppm for PTMC and 3.07 ppm for LrPC) and the end group peaks (5.12 ppm (**i**) for BnOH and 5.42 ppm (**e'**) for *o*-nitrobenzyl carbamate end groups, respectively) in ^{1}H NMR spectra. In addition, differing from LrM the obtained light-responsive homo- and copolycarbonates are soluble in common organic solvents, such as acetone, DCM, DMSO, DMF, THF and MeCN.

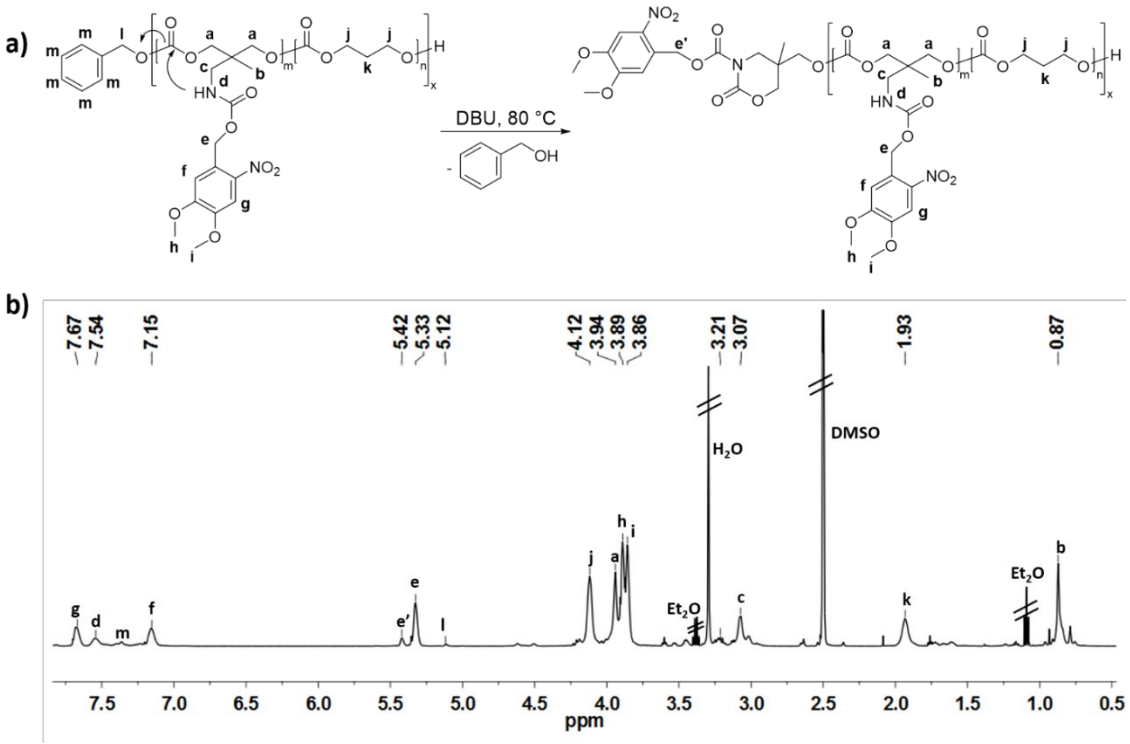

Figure 4. a) Transcarbamation side reaction catalyzed by DBU during the ROP; b) ^{1}H NMR spectrum of **LrPC-2**

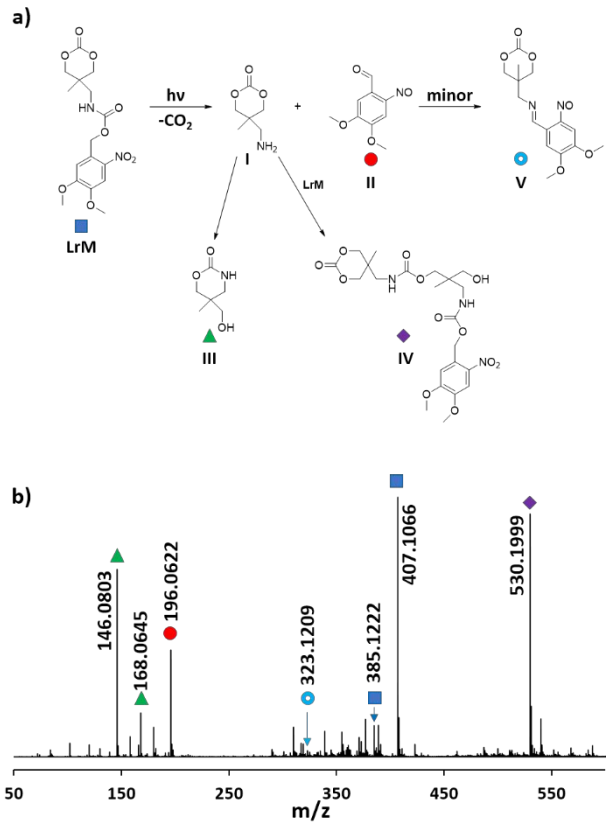

Figure 5. a) Degradation mechanism of **LrM** upon irradiation. b) ESI-ToF mass spectrum for degradation products of **LrM** after irradiation (320 – 480 nm, 0.607 W/cm^2) for 15 min. [**III**+H]$^+$, calcd: 146.0812, found: 146.0803; [**III**+Na]$^+$, calcd: 168.0631, found: 168.0645; [**II**+H]$^+$, calcd: 196.0604, found: 196.0622; [**V**+H]$^+$, calcd: 323.1238, found: 323.1209; [**LrM**+H]$^+$, calcd: 385.1242, found: 385.1222; [**LrM**+Na]$^+$, calcd: 407.1061, found: 407.1066; [**IV**+H]$^+$, calcd: 530.1980, found: 530.1999.

Light degradation study of LrM followed by ESI-ToF-MS and NMR. To clearly determine the degradation products, **LrM** was irradiated with UV light (320 – 480 nm, 0.607 W/cm^2) for 15 min and studied by ESI-ToF-MS. As shown in **Figure 5**, upon irradiation **LrM** was decomposed as expected into an intermediate 5-(aminomethyl)-5-methyl-1,3-dioxan-2-one (**I**) and 4,5-

dimethoxy-2-nitrosobenzaldehyde (**II**) via a radical reduction mechanism, which has been discussed elsewhere[49,50]. The reactive intermediate **I** transformed then into the thermally stable six-membered cyclic carbamate **III** *via* intramolecular transcarbamation of the functional amine group with the carbonate group. Since **LrM** was irradiated in the suspension state, differing from other previously published works[18], we observed the intermolecular degradation product **IV** as well. In the presence of **LrM**, **IV** was formed by the intermolecular ring-opening reaction of **I** with **LrM**. In addition, it was well known that the condensation reaction between primary amine and aldehyde leads to the formation of imine functionalities. Imine **V** could be detected as a minor degradation product generated from amine **I** and aldehyde **II**. The proton NMR analysis (**Figure S16**) showed that, after irradiation for 15 min 91% 4,5-dimethoxy-2-nitrobenzyl group has been cleaved based on the significant signal reduction of the benzylic CH_2 group at 5.35 ppm. The remaining signals indicated the emergence of aldehyde, alcohol and cyclic carbamate.

Change in absorbance of LrPC-2 upon irradiation. As shown in **Figure 6a**, the photoisomerization of 4,5-dimethoxy-2-nitrobenzyl group was carried out upon irradiation with UV light into an *o*-nitrosobenzylaldehyde leading to release of a free amine pendent group. To follow the deprotection rate, the absorbance changes of **LrPC-2** in DCM (0.075 mg/mL) were investigated by employing a UV/VIS spectrophotometer. Upon irradiation the absorbance at 346 nm decreased due to the cleavage of 4,5-dimethoxy-2-nitrobenzyl light-sensitive protecting group, while a new absorbance appeared at 430 nm, which could be assigned to the degradation product of 4,5-dimethoxy-2-nitrosobenzaldehyde. The UV/VIS spectrum remained unchanged after irradiation for 180 s indicating complete cleavage of protecting group from polymer side chains.

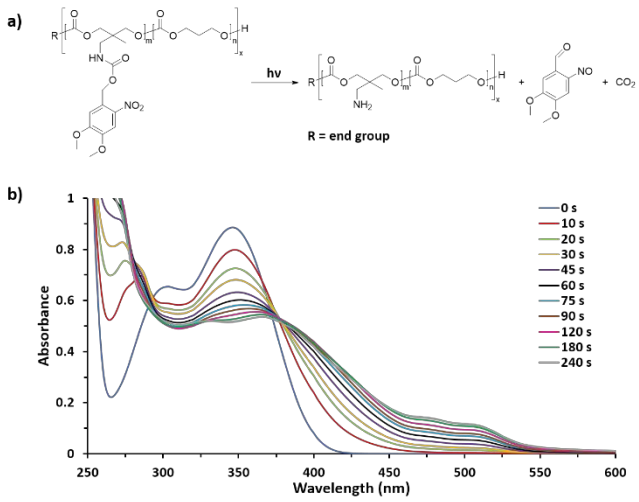

Figure 6. a) Cleavage of 4,5-dimethoxy-2-nitrobenzyl protecting group from **LrPC-2** upon irradiation with UV light. b) Change of the UV/VIS absorbance of **LrPC-2** in DCM (0.075 mg/mL) upon irradiation with UV light (320 – 480 nm, 0.607 W/cm^2) for various irradiation times up to 180 s.

Light degradation study of LrPC-2 followed by SEC. The light degradation of **LrPC-2** in dependence on the irradiation time (0.607 W/cm^2, 320 – 480 nm for 0, 1, 5, 15, 30 min) was analysed by SEC. As designed the residual amino function formed upon irradiation initiated the polymer degradation by a subsequent intramolecular cyclization. In **Figure 7** is shown that the degradation strongly depends on the time of irradiation. In this case a shift of the high molar mass peak maximum can be observed, which indicates the cleavage of the light-responsive side groups. At the same time, the peak area decreased, which is proportional to the number of polymer chains. This means that the degradation of the chain took place immediately after the side chain is split off, which suggests a rapid intramolecular reaction. The longer the sample was exposed to the UV light, the more the molecular weight decreased and the portion of the degradation products (elution

time 2.3 to 2.6 min in **Figure 7**) increased. Irradiation times longer than 15 min did not show much differences in the molecular weight and elugramm. Hence, it can be assumed that the degradation was finished within 15 min. The degradation products are oligomers with M_n less than 1,000 g/mol. All samples were measured immediately after irradiation, it is therefore clear that the polymer degradation occurred only during the irradiation time, and was not propagated beyond. The degree of degradation can thus be controlled well by the duration of the exposure.

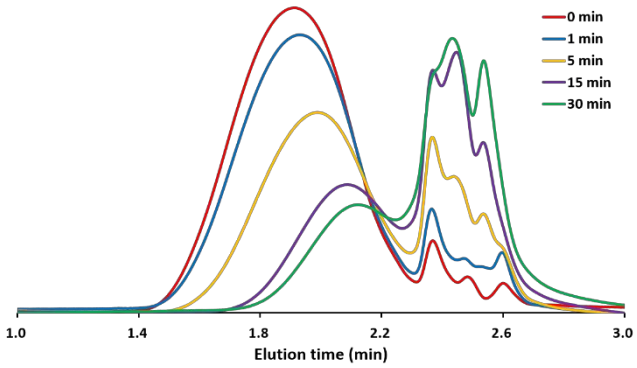

Figure 7. SEC traces of **LrPC-2** after exposure to UV light (320 – 480 nm, 0.607 W/cm^2) for 0, 1, 5, 15, or 30 min.

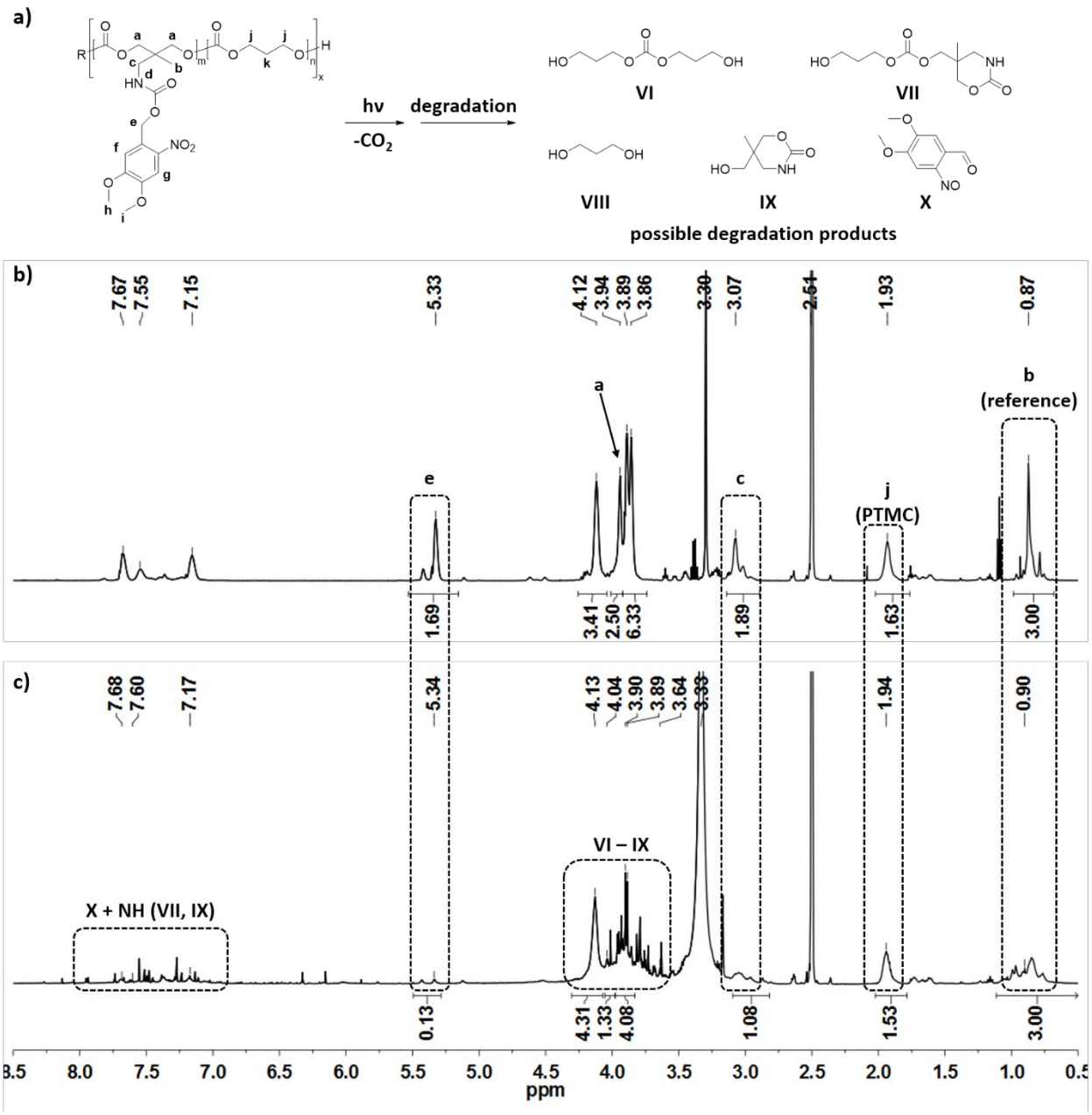

Figure 8. a) Light degradation of **LrPC-2** and ^{1}H NMR spectra of **LrPC-2** before (b) and after (c) exposure to UV light (320 – 480 nm, 0.607 W/cm^2) for 15 min

Light degradation study of LrPC-2 followed by NMR spectroscopy. The light degradation of **LrPC-2** and its degradation products were monitored by ^{1}H NMR spectroscopy in DMSO-d_6 solution. The ^{1}H NMR spectra before and after exposure to UV light (320 – 480 nm, 0.607 W/cm^2) for 15 min are shown in **Figure 8**. The signal of CH_3(**b**) was used as reference, because the relative intensity of CH_3(**b**) should remain unchanged during the degradation process. Upon irradiation for 15 min the relative intensity of characteristic NMR peak corresponding to the CH_2 (**e**, 5.33 ppm) decreased from 1.69 to 0.13 indicating about 92% cleavage of the light-sensitive 4,5-dimethoxy-2-nitrobenzyl groups. As a result of the subsequent intramolecular cyclization the peak at 3.94 ppm (**a**) corresponding to the both CH_2 groups in **LrPC** decreased significantly and changed from broad peak to sharper small molecule peaks. The newly generated sharper signals between 3.50 and 4.25 ppm could be assigned to the methyl protons connected with carbonate, alcohol and carbamate functional groups of possible degradation products **VI** – **IX**. Another major change was the disappear of signals between 7.0 and 8.0 ppm corresponding to the 4,5-dimethoxy-2-nitrobenzyl (**f** and **g**) and carbamate (**d**) groups, and the formation of sharper monomer peaks (**VII**, **IX** and **X**) indicating the successful cleavage of light-responsive pendent chains.

Nanoparticle preparation and characterization. A solvent displacement method was used to generate NP in a size range of about 100 nm. As can be seen in **Table 2**, all formulations prepared by the solvent displacement method were obtained with the aimed hydrodynamic diameters, with values between 100 nm and 126 nm.

All systems were obtained as monodisperse samples with PDI values below 0.1. The measured zeta potentials were all negative (-16 mV to -31 mV). Regarding their physicochemical characteristics, almost no difference between unloaded NP and PS-loaded NP was detected. Photosensitizer containing NP achieved drug load values between 50 and 67 µg *m*THPC/mg NP.

Table 2. Physicochemical characteristics of different unloaded and *m*THPC-loaded nanoparticles (mean ± SD; n ≥ 3).

Nanoparticle system	Hydrodynamic diameter (nm)	PDI	Zetapotential (mV)	Drug load (µg *m*THPC/mg NP)
PLGA-NP	100.6 ± 5.2	0.09 ± 0.01	-31.0 ± 6.2	-
*m*THPC-PLGA-NP	125.5 ± 0.6	0.06 ± 0.02	-16.2 ± 4.6	50.5 ± 1.5
LrPC-PLGA-NP	108.9 ± 6.9	0.07 ± 0.03	-21.2 ± 0.8	-
*m*THPC-LrPC-PLGA-NP	109.3 ± 4.1	0.08 ± 0.01	-29.2 ± 1.2	67.4 ± 13.7

Nanoparticle degradation and drug release. As described above, the **LrPC** used for the nanoparticle preparation showed a light-induced degradation before its manufacturing into particle matrices. To investigate, whether the polymer retained its degradation properties after processing to nanoformulations, the PCS count rate of nanosuspensions based on pure PLGA polymer (PLGA-NP) and a mixture of 25% **LrPC** and 75% PLGA (LrPC-PLGA-NP) was measured. The particle suspension (0.1 mg NP/mL) was irradiated with low level UV light of a wavelength of 365 nm (Thorlabs´ Mounted LED M365LP1, 1,150 mW, Ø57.0 mm, 1.76 mW/cm^2) for 5 min. The count rate thereby reflects the average scattering intensity during the PCS measurements. Under specified conditions such as a fixed particle size, it is a representative for the nanoparticle concentration in the sample. **Figure 9** shows the light-dependent variation of the count rate of LrPC-PLGA-NP in comparison to light-insensitive PLGA-NP, before, and over a period of 24 h after illumination. As illustrated, the tested **LrPC**-containing formulation showed degradation behaviour over the observed time. Directly after illumination, the count rate decreased from 100% to 77.2% and after further 24 h of incubation without illumination an additional count rate decreases of about 30% was measured. In contrast to these findings, PLGA-NP, not containing the

light-cleavable **LrPC** polymer, showed no light-dependent degradation. The count rate remained constant at approximately 100% over 24 h.

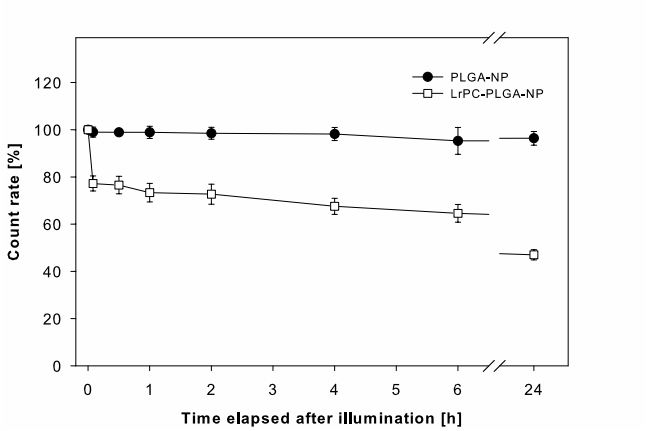

Figure 9. Variation of the count rate as parameter for nanoparticle degradation over time. Light-cleavable NP (LrPC-PLGA-NP) were compared to a light-insensitive particle system (PLGA-NP), up to 24 h after illumination (mean ± SD; n = 3).

To ensure that PS incorporation does not affect the nanoparticle degradation properties, AFM measurements of *m*THPC-LrPC-PLGA-NP before and after illumination were conducted. As shown in **Figure 10**, the non-illuminated sample showed spherical nanoparticles with an average hydrodynamic diameter of about 100 nm. These results were comparable to the PCS measurement results described above (**Table 2**). After 5 min of illumination and 24 h rest time in the dark at room temperature, the quantity and shape of the formulations changed. The number of detected nanoparticles decreased while remaining particles formed agglomerates. Hence, the visualization of illumination-triggered nanoparticle breakdown and structural change demonstrated the functionality of the light-responsive *m*THPC-LrPC-PLGA-NP.

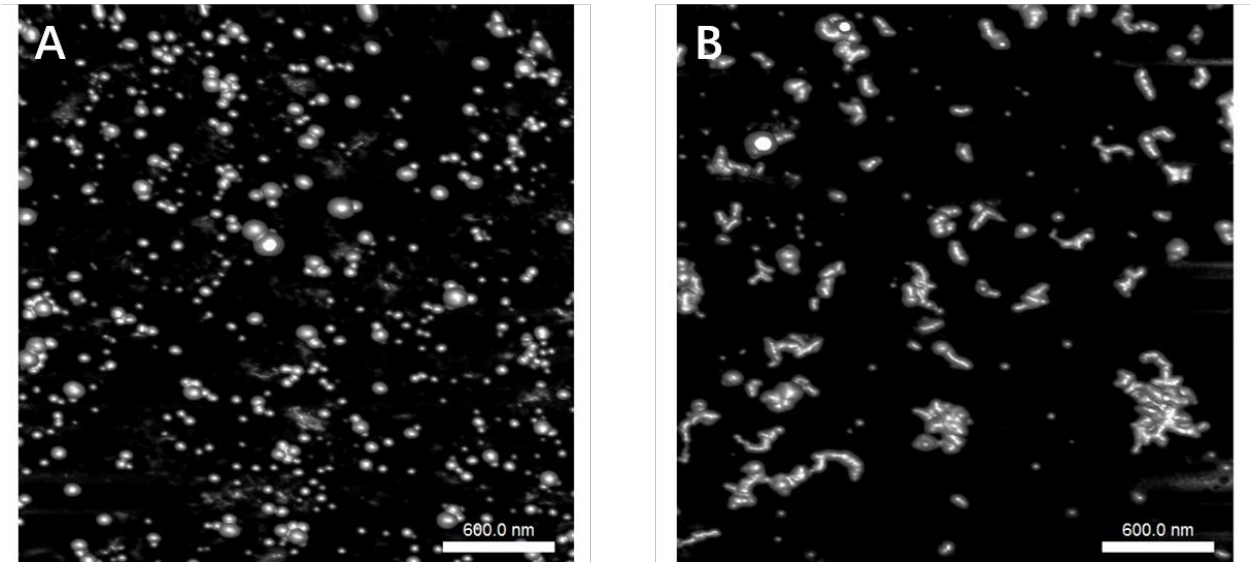

Figure 10. Visualization of nanoparticle morphology of *m*THPC-LrPC-PLGA-NP via atomic force microscopy. Nanoparticle samples were investigated (A) before and (B) 24 h after illumination.

The conducted *in vitro* release studies confirmed the hypothesis, that illumination of the manufactured systems leads to increased drug release. Observing the drug release kinetics over the investigated time period of 24 h after illumination, the differences between both tested formulations became clear. As depicted in **Figure 11**, the nanoparticles containing the light-responsive LrPC polymer showed a significant drug release with remarkable increases of released *m*THPC within the first hour after illumination. On the other hand, the light-insensitive formulation showed only a very limited drug leakage of about 10% over the same time period.

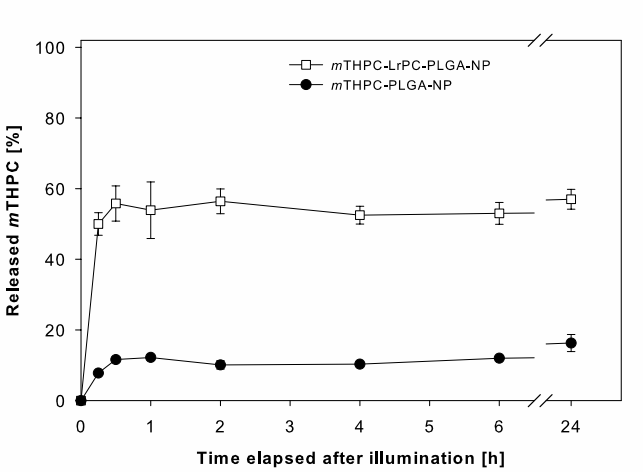

Figure 11. Temoporfin release profile of light-cleavable nanoparticles (LrPC-PLGA-NP) compared to a light-insensitive particle system (PLGA-NP) over a time period of 24 h (mean ± SD; n = 3).

Taking the results together, the proposed LrPC polymer in combination with PLGA could be used as starting material for the preparation of well-defined nanoparticles. An effective nanoparticle degradation after even low level of illumination with light of 365 nm could be achieved leading to a pronounced drug release of temoporfin in comparison to light-insensitive nanoparticles prepared on the basis of pure PLGA polymer.

CONCLUSIONS

In conclusion, we have prepared a novel light-responsive poly(trimethylene carbonate)-based aliphatic copolycarbonate (**LrPC**) with pendent 4,5-dimethoy-2-nitrobenzyl group by DBU

catalysed ROP. Based on the kinetic investigation the ROP of TMC and **LrM** provided a copolycarbonate with M_n of 4,400 g/mol, $Đ_M$ of 1.47 and about 50% light-responsive part. Upon irradiation with UV light the copolycarbonate degraded rapidly and completely into oligomers or small molecules, which were confirmed by NMR, SEC and UV/VIS measurements. Stable monodisperse nanoparticles with hydrodynamic diameter of 100 nm determined by PCS could be formulated from 25% **LrPC** and 75% PLGA. After irradiation of the particle suspension for 5 min with UV light, a significant decrease of the particle count rate was observed indicating that the obtained nanoparticles retained degradation properties, while the standard PLGA nanoparticles remained stable. These nanoparticles were employed for the encapsulation of photosensitizer (temoporfin) payload. Mixing only 25% **LrPC** into PLGA nanoparticles could significantly increase the release rate of temoporfin upon irradiation after low level of illumination with light of 365 nm in comparison to standard PLGA nanoparticles. This work demonstrated that combination of encapsulation of photosensitizer and light degradation using light-responsive polymers is suitable to enhance photodynamic therapy (PDT).

ASSOCIATED CONTENT

Supporting Information.

The following files are available free of charge.

Characterization (NMR, DSC and ESI-ToF-MS) of small molecules and polymers; Determination of monomer conversions by NMR spectroscopy; Additional figures for the

kinetic investigation of (co)polymerization and polymer stability investigation. Additional ^{1}H NMR spectra for the light degradation of LrM.

AUTHOR INFORMATION

Corresponding Author

*Dirk Kuckling, Email: dirk.kuckling@uni-paderborn.de; Tel +49 5251 60-2171; Fax +49 5251 60-3245.

ACKNOWLEDGMENT

The authors gratefully acknowledge financial support from the German Ministry of Education and Research (GITCare 13N13425 and 13N13423). The authors thank Waters Corporation for the support of ACQUITY Advanced Polymer Chromatography (APC) system. S. Schreiber and Dr. F. Herrmann, Institute for Pharmaceutical Biology and Phytochemistry, University of Münster, are gratefully acknowledged for AFM measurements.

REFERENCES

1. Yuen, A. Y.; Lopez-Martinez, E.; Gomez-Bengoa, E.; Cortajarena, A. L.; Aguirresarobe, R. H.; Bossion, A.; Mecerreyes, D.; Hedrick, J. L.; Yang, Y. Y.; Sardon, H. Preparation of Biodegradable Cationic Polycarbonates and Hydrogels through the Direct Polymerization of Quaternized Cyclic Carbonates. *ACS Biomater. Sci. Eng.* **2017,** *3* (8), 1567-1575.

2. Chesterman, J. P.; Chen, F.; Brissenden, A. J.; Amsden, B. G. Synthesis of cinnamoyl and coumarin functionalized aliphatic polycarbonates. *Polym. Chem.* **2017,** *8* (48), 7515-7528.

3. Wright, K. J.; Badwaik, V. D.; Samaddar, S.; Hyun, S.-H.; Glauninger, K.; Eom, T.; Thompson, D. H. Organocatalytic Synthesis and Evaluation of Polycarbonate Pendant Polymer: β-Cyclodextrin-Based Nucleic Acid Delivery Vectors. *Macromolecules* **2018,** *51* (3), 670-678.

4. Sun, J.; Kuckling, D. Synthesis of high-molecular-weight aliphatic polycarbonates by organo-catalysis. *Polym. Chem.* **2016,** *7* (8), 1642-1649.

5. Sun, J.; Aly, K. I.; Kuckling, D. A novel one-pot process for the preparation of linear and hyperbranched polycarbonates of various diols and triols using dimethyl carbonate. *RSC Adv.* **2017,** *7* (21), 12550-12560.

6. Sun, J.; Aly, K. I.; Kuckling, D. Synthesis of hyperbranched polymers from vegetable oil based monomers via ozonolysis pathway. *J. Polym. Sci., Part A: Polym. Chem.* **2017,** *55* (12), 2104-2114.

7. Sudakar, P.; Sivanesan, D.; Yoon, S. Copolymerization of Epichlorohydrin and CO_2 Using Zinc Glutarate: An Additional Application of ZnGA in Polycarbonate Synthesis. *Macromol. Rapid Commun.* **2016,** *37* (9), 788-793.

8. Meng, Q.; Pepper, K.; Cheng, R.; Howdle, S. M.; Liu, B. Effect of supercritical CO_2 on the copolymerization behavior of cyclohexene oxide/CO_2 and copolymer properties with DMC/Salen-Co(III) catalyst system. *J. Polym. Sci., Part A: Polym. Chem.* **2016,** *54* (17), 2785-2793.

9. Sun, J.; Fransen, S.; Yu, X.; Kuckling, D. Synthesis of pH-cleavable poly(trimethylene carbonate)-based block copolymers via ROP and RAFT polymerization. *Polym. Chem.* **2018,** *9* (23), 3287-3296.

10. Yildirim, I.; Sungur, P.; Crecelius-Vitz, A. C.; Yildirim, T.; Kalden, D.; Hoeppener, S.; Westerhausen, M.; Weber, C.; Schubert, U. S. One-pot synthesis of PLA-b-PHEA via sequential

ROP and RAFT polymerizations. *Polym. Chem.* **2017,** *8* (39), 6086-6098.

11. Dai, Y.; Zhang, X. Recent development of functional aliphatic polycarbonates for the construction of amphiphilic polymers. *Polym. Chem.* **2017,** *8* (48), 7429-7437.

12. Saito, T.; Aizawa, Y.; Yamamoto, T.; Tajima, K.; Isono, T.; Satoh, T. Alkali Metal Carboxylate as an Efficient and Simple Catalyst for Ring-Opening Polymerization of Cyclic Esters. *Macromolecules* **2018,** *51* (3), 689-696.

13. Lingier, S.; Spiesschaert, Y.; Dhanis, B.; Wildeman, S. D.; Prez, F. E. D. Rigid Polyurethanes, Polyesters, and Polycarbonates from Renewable Ketal Monomers. *Macromolecules* **2017,** *50* (14), 5346-5352.

14. Zelikin, A. N.; Putnam, D. Poly(carbonate-acetal)s from the Dimer Form of Dihydroxyacetone. *Macromolecules* **2005,** *38* (13), 5532-5537.

15. Snyder, R. L.; Fortman, D. J.; Hoe, G. X. D.; Hillmyer, M. A.; Dichtel, W. R. Reprocessable Acid-Degradable Polycarbonate Vitrimers. *Macromolecules* **2018,** *51* (2), 389-397.

16. Xia, Y.; Zeng, Y.; Hu, D.; Shen, H.; Deng, J.; Lu, Y.; Xia, X.; Xu, W. Light and pH dual-sensitive biodegradable polymeric nanoparticles for controlled release of cargos. *J. Polym. Sci., Part A: Polym. Chem.* **2017,** *55* (10), 1773-1783.

17. Xie, M.; Yu, L.; Li, Z.; Zheng, Z.; Wang, X. Synthesis and character of novel polycarbonate for constructing biodegradable multi-stimuli responsive delivery system. *J. Polym. Sci., Part A: Polym. Chem.* **2016,** *54* (22), 3583-3592.

18. Qiu, F.; Zhang, M.; Du, F.; Li, Z. Oxidation Degradable Aliphatic Polycarbonates with Pendent Phenylboronic Ester. *Macromolecules* **2017,** *50* (1), 23-34.

19. Qiu, F.; Song, C.; Zhang, M.; Du, F.; Li, Z. Oxidation-Promoted Degradation of Aliphatic Poly(carbonate)s via Sequential 1,6-Elimination and Intramolecular Cyclization. *ACS Macro Lett.*

2015, *4* (11), 1220-1224.

20. Wang, Y.; Ke, X.; Voo, Z. X.; Yap, S. S. L.; Yang, C.; Gao, S.; Liu, S.; Venkataraman, S.; Obuobi, S. A. O.; Khara, J. S.; Yang, Y. Y.; Ee, P. L. R. Biodegradable functional polycarbonate micelles for controlled release of amphotericin B. *Acta Biomater.* **2016,** *46*, 211-220.

21. Shen, H.; Xia, Y.; Qin, Z.; Wu, J.; Zhang, L.; Lu, Y.; Xia, X.; Xu, W. Photoresponsive biodegradable poly(carbonate)s with pendent o-nitrobenzyl ester. *J. Polym. Sci., Part A: Polym. Chem.* **2017,** *55* (17), 2770-2780.

22. Henn, D. M.; Lau, C. M.; Lib, C. Y.; Zhao, B. Light-triggered unfolding of single linear molecular bottlebrushes from compact globular to wormlike nano-objects in water. *Polym. Chem.* **2017,** *8* (17), 2702-2712.

23. Wendler, F.; Schneider, K. R. A.; Dietzek, B.; Schacher, F. H. Light-responsive terpolymers based on polymerizable photoacids. *Polym. Chem.* **2017,** *8* (19), 2959-2971.

24. Durand, P.; Brege, A.; Chollet, G.; Grau, E.; Cramail, H. Simple and Efficient Approach toward Photosensitive Biobased Aliphatic Polycarbonate Materials. *ACS Macro Lett.* **2018,** *7* (2), 250-254.

25. Manavitehrani, I.; Fathi, A.; Badr, H.; Daly, S.; Shirazi, A. N.; Dehghani, F. Biomedical applications of biodegradable polyesters. *Polymers* **2016,** *8* (1), 1-32.

26. Lux, C. d. G.; McFearin, C. L.; Joshi-Barr, S.; Sankaranarayanan, J.; Fomina, N.; Almutairi, A. Single UV or Near IR Triggering Event Leads to Polymer Degradation into Small Molecules. *ACS Macro Lett.* **2012,** *1* (7), 922-926.

27. DiLauro, A. M.; Robbins, J. S.; Phillips, S. T. Reproducible and Scalable Synthesis of End-Cap-Functionalized Depolymerizable Poly(phthalaldehydes). *Macromolecules* **2013,** *46* (8), 2963-2968.

28. DiLauro, A. M.; Zhang, H.; Baker, M. S.; Wong, F.; Sen, A.; Phillips, S. T. Accessibility of Responsive End-Caps in Films Composed of Stimuli-Responsive, Depolymerizable Poly(phthalaldehydes). *Macromolecules* **2013,** *46* (18), 7257-7265.

29. June, S. M.; Suga, T.; Heath, W. H.; Lin, Q.; Puligadda, R.; Yan, L.; Dillard, D.; Long, T. E. Photoactive polyesters containing o-nitro benzyl ester functionality for photodeactivatable adhesion. *J. Adhes.* **2013,** *89* (7), 548-558.

30. Fomina, N.; McFearin, C.; Sermsakdi, M.; Edigin, O.; Almutairi, A. UV and Near-IR Triggered Release from Polymeric Nanoparticles. *J. Am. Chem. Soc.* **2010,** *132* (28), 9540-9542.

31. Lux, C. d. G.; Almutairi, A. Intramolecular Cyclization for Stimuli-Controlled Depolymerization of Polycaprolactone Particles Leading to Disassembly and Payload Release. *ACS Macro Lett.* **2013,** *2* (5), 432-435.

32. Olejniczak, J.; Chan, M.; Almutairi, A. Light-Triggered Intramolecular Cyclization in Poly(lactic-co-glycolic acid)-Based Polymers for Controlled Degradation. *Macromolecules* **2015,** *48* (10), 3166-3172.

33. Meng, Z.; Hou, W.; Zhou, H.; Zhou, L.; Chen, H.; Wu, C. Therapeutic Considerations and Conjugated Polymer-Based Photosensitizers for Photodynamic Therapy. *Macromol. Rapid Commun.* **2017,** *39* (5), 1700614.

34. Jung, H. S.; Verwilst, P.; Sharma, A.; Shin, J.; Sessler, J. L.; Kim, J. S. Organic molecule-based photothermal agents: an expanding photothermal therapy universe. *Chem. Soc. Rev.* **2018,** *47* (7), 2280-2297.

35. Ding, X.; Liu, J.; Li, J.; Wang, F.; Wang, Y.; Song, S.; Zhang, H. Polydopamine coated manganese oxide nanoparticles with ultrahigh relaxivity as nanotheranostic agents for magnetic resonance imaging guided synergetic chemo-/photothermal therapy. *Chem. Sci.* **2016,** *7* (11),

6695-6700.

36. Jeong, K.; Kang, C. S.; Kim, Y.; Lee, Y. D.; Kwon, I. C.; Kim, S. Development of highly efficient nanocarrier-mediated delivery approaches for cancer therapy. *Cancer Lett.* **2016,** *374* (1), 31-43.

37. Xu, L.; Zhao, M.; Yang, Y.; Liang, Y.; Sun, C.; Gao, W.; Li, S.; He, B.; Pu, Y. A reactive oxygen species (ROS)-responsive low molecular weight gel co-loaded with doxorubicin and Zn(II) phthalocyanine tetrasulfonic acid for combined chemo-photodynamic therapy. *J. Mater. Chem. B* **2017,** *5* (46), 9157-9164.

38. Wong, R. C. H.; Ng, D. K. P.; Fong, W. P.; Lo, P. C. Encapsulating pH-responsive doxorubicin-phthalocyanine conjugates in mesoporous silica nanoparticles for combined photodynamic therapy and controlled chemotherapy. *Chem. Eur. J.* **2017,** *23* (65), 16505-16515.

39. Jia, Z.; Lonsdale, D. E.; Kulis, J.; Monteiro, M. J. Construction of a 3-Miktoarm Star from Cyclic Polymers. *ACS Macro Lett.* **2012,** *1* (6), 780-783.

40. Gash, V. W. Dienoalkyl ethers. General synthesis of the symmetrical ethers. *J. Org. Chem.* **1972,** *37* (13), 2197-2201.

41. Liu, S. T.; Liu, C. Y. Synthesis of amino-containing phosphines. The use of iminophosphorane as a protecting group for primary amines. *J. Org. Chem.* **1992,** *57* (22), 6079-6080.

42. Ure, A. D.; Lázaro, I. A.; Cottera, M.; McDonald, A. R. Synthesis and characterisation of a mesocyclic tripodal triamine ligand. *Org. Biomol. Chem.* **2016,** *14* (2), 483-494.

43. Liu, J.; Liu, W.; Weitzhandler, I.; Bhattacharyya, J.; X. Li, J. W.; Qi, Y.; Bhattacharjee, S.; Chilkoti, A. ring-opening polymerization of prodrugs: A versatile approach to prepare well-defined drug-loaded nanoparticles. *Angew. Chem. Int. Ed.* **2015,** *54* (3), 1002-1006.

44. Lohmeijer, B. G. G.; Pratt, R. C.; Leibfarth, F.; Logan, J. W.; Long, D. A.; Dove, A. P.; Nederberg, F.; Choi, J.; Wade, C.; Waymouth, R. M.; Hedrick, J. L. Guanidine and amidine organo-catalysts for ring-opening polymerization of cyclic esters. *Macromolecules* **2006,** *39* (25), 8574-8583.

45. Pounder, R. J.; Dove, A. P. Synthesis and Organocatalytic Ring-Opening Polymerization of Cyclic Esters Derived from L-Malic Acid. *Biomacromolecules* **2010,** *11* (8), 1930-1939.

46. Nederberg, F.; Lohmeijer, B. G. G.; Leibfarth, F.; Pratt, R. C.; Choi, J.; Dove, A. P.; Waymouth, R. M.; Hedrick, J. L. Organocatalytic Ring Opening Polymerization of Trimethylene Carbonate. *Biomacromolecules* **2007,** *8* (1), 153-160.

47. Endo, T.; Kakimoto, K.; Ochiai, B.; Nagai, D. Synthesis and Chemical Recycling of a Polycarbonate Obtained by Anionic Ring-Opening Polymerization of a Bifunctional Cyclic Carbonate. *Macromolecules* **2005,** *38* (20), 8177-8182.

48. Matsuo, J.; Aoki, K.; Sanda, F.; Endo, T. Substituent Effect on the Anionic Equilibrium Polymerization of Six-Membered Cyclic Carbonates. *Macromolecules* **1998,** *31* (14), 4432-4438.

49. Il'ichev, Y. V.; Schwörer, M. A.; Wirz, J. Photochemical Reaction Mechanisms of 2-Nitrobenzyl Compounds: Methyl Ethers and Caged ATP. *J. Am. Chem. Soc.* **2004,** *126* (14), 4581-4595.

50. Pelliccioli, A. P.; Wirz, J. Photoremovable protecting groups: reaction mechanisms and applications. *Photochem. Photobiol. Sci.* **2002,** *1* (7), 441-458.

Use of light-degradable aliphatic polycarbonate nanoparticles as drug carrier for photosensitizer

Jingjiang Sun[†//], *Wolfgang Birnbaum*[†], *Juliane Anderski*[‡], *Marie-Theres Picker*[†], *Dennis Mulac*[‡], *Klaus Langer*[‡], *Dirk Kuckling*[†]*

TABLE OF CONTENTS